ITER Hybrid and Steady State Scenario Modeling

A.H. Kritz[1], C. Kessel[2], G. Bateman[1], T. Rafiq[1]
D.C. McCune[2], R.V. Budny[2], A.Y. Pankin[1]
[1] *Department of Physics, Lehigh University, Bethlehem, PA 18015, United States*
[2] *PPPL, Princeton University, PO Box 451, Princeton, NJ 08543, United States*

Detailed scenario modeling is carried out for two different kinds of ITER discharges, hybrid discharges and steady state discharges. The objective of the modeling is to prepare for the commissioning of ITER and to plan for the burn stages of ITER operation. The hybrid discharges are H-mode discharges with a lower plasma current than the plasma current in the standard ELMy H-mode discharges. In the standard H-mode scenario, the plasma current, I_p, is 15 MA and the plasma line average density, $n_{e0,20} \approx 1.0$, is close to the Greenwald limit during the flat-top burn stage of the discharge [1]. In the hybrid discharge simulations described in this paper, a lower plasma current is employed, $I_p = 12.5$ MA, in order to avoid sawtooth oscillations and obtain enhanced confinement at reduced current in H-mode. The plasma density, $n_{e,20} = 0.86$, is correspondingly lower than in the 15 MA H-mode discharge. In contrast, in the steady state discharges considered, the current is lower, $I_p = 9$ MA, with a correspondingly lower plasma density, $n_{e,20} = 0.55$ - 0.78. In the steady state discharges all of the plasma current is driven by auxiliary heating and bootstrap current drive.

Simulations are carried out utilizing a combination of two full-featured integrated modeling codes, the Tokamak Simulation Code (TSC) and the PTRANSP code. The TSC code is used to compute free-boundary equilibria together with corresponding coil currents during the evolution of the plasma from start-up to shut down. The time dependent plasma shape and density profiles are passed to the PTRANSP code, which computes current drive and power deposition profiles as well as toroidal angular rotation profiles in either analysis or predictive mode. The resulting plasma profiles are passed back to the TSC code in order to converge on complete self-consistent simulations for each type of ITER discharge. The TSC simulations use the Coppi-Tang transport model, modified for the simulation of internal transport barriers. The predictive PTRANSP simulations are carried out using a new version of the Multi-Mode transport model, which includes a drift resistive inertial ballooning component, or the GLF23 transport model.

Auxiliary heating sources are computed in PTRANSP using the NUBEAM module for neutral beam injection, the TORIC full wave module for ICRF, the LSC 1-D Fokker

Planck module for lower hybrid, and the TORAY module for electron cyclotron heating and current drive. Fusion reaction rates and atomic physics cross sections for ionization, recombination and impurity radiation are computed using the ADAS module [2], which is a recently added feature in the PTRANSP code. The value used for the height of the pedestal temperature, 5 keV, is based on results obtained using the EPED1 model [3]. The NCLASS module is used to compute neoclassical ion thermal transport as well as neoclassical resistivity and bootstrap current for the evolution of the magnetic q profile. The KDSAW module is used to compute the effect of sawtooth crashes, when conditions are appropriate for sawtooth oscillations.

In the ITER scenario simulations, the evolution of the plasma discharge is followed from the early start-up stage, with plasma current as low as 0.5 MA and correspondingly low density, to full current and density during the flat-top burn stage. The ramp-up stage of the discharge is approximately 150 seconds for the hybrid H-mode and steady state discharges considered. Various levels of heating are used during the ramp-up stages in order to freeze in a broad current density profile. The intent is to avoid or delay sawtooth oscillations, by maintaining $q_{axis} > 1$, or to produce a reversed magnetic shear configuration for the steady state discharges. Feedback loops are used in the TSC code to control the plasma position and shape while constraints are used for the maximum allowed coil currents. The time evolution of the plasma boundary position and shape, just inside the separatrix, is passed from the TSC code to the PTRANSP code, in which the prescribed-boundary version of the TEQ module is used to compute the self-consistent evolution of the equilibrium. (The equilibrium module and many of the modules used in the PTRANSP code are available at the site http://w3.pppl.gov/NTCC/.)

Contributions to the total plasma current in the hybrid discharge (12.45 MA) and in the steady state discharge (9.0 MA) are shown in Figs. 1 and 2 as a function of time. These results are obtained in the PTRANSP analyses of TSC simulations. It can be seen that the bootstrap current provides the largest contribution to the non-inductive current in both scenarios (2.8 MA for the hybrid discharge and 5.2 MA for the steady state discharge). The bootstrap current accounts for more than half of the current drive in the steady state scenario. Nearly two thirds of the current in the hybrid scenario is inductively driven while there is no inductive current after the initial stages of the steady state scenario. The current, other than bootstrap current, is driven by neutral beam and lower hybrid heating. In Figs. 1 and 2, it is shown that the discharges are simulated from the low current start up stage well into the flat-top burn phase of the discharge.

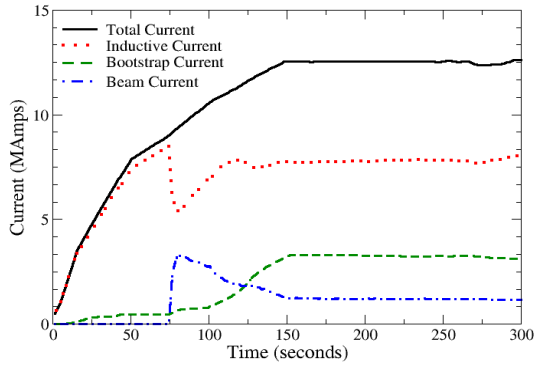

Figure 1 Hybrid discharge: Current vs Time

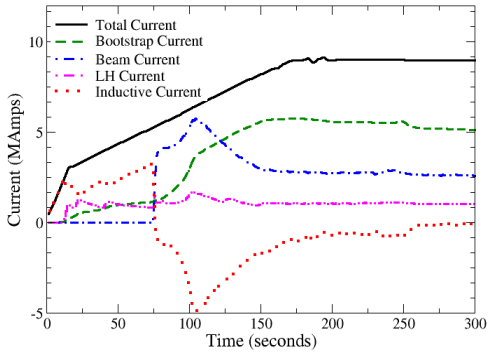

Figure 2 Steady state dischrge: Current vs Time

In simulations carried out using the PTRANSP code, effects associated with varying the orientation of the neutral beams and the ion cyclotron frequency are examined. Two 1 MeV beams each inject 16.5 MW of power into the plasma in the steady state discharge. Three scenarios are considered. In one, both beams are directed toward the plasma center, in the second scenario one beam is directed toward the plasma center and the other is directed off-center, and in a third scenario both beams are directed away from the plasma center. The beam-driven current density in each of these cases is shown in Fig. 3 for the steady state discharge. As a consequence of the area dependence on radius, it is seen in Fig. 4 that the total current deposited within a given radius is nearly independent of the beam steering. The dependence of power deposition on the ion cyclotron frequency is illustrated in Fig. 5 where the deposited power density is plotted as a function of major radius for two values of ICRF frequency. It is seen that as the frequency increases, the resonance shifts to the region of higher magnetic field so that the power deposition is less centrally deposited and instead is deposited at a smaller major radius.

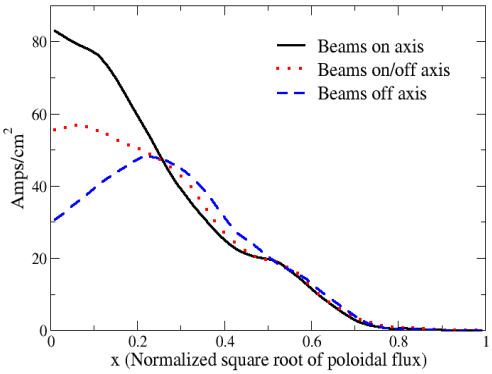

Figure 3 Dependence of driven current on beam steering

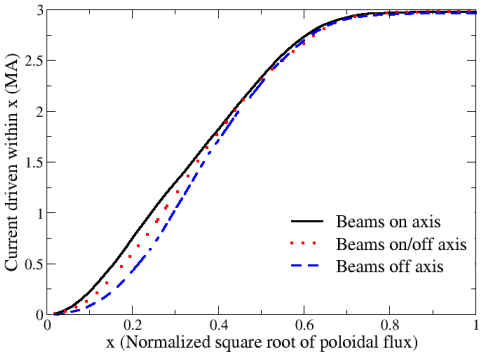

Figure 4 Accumulated current versus radius

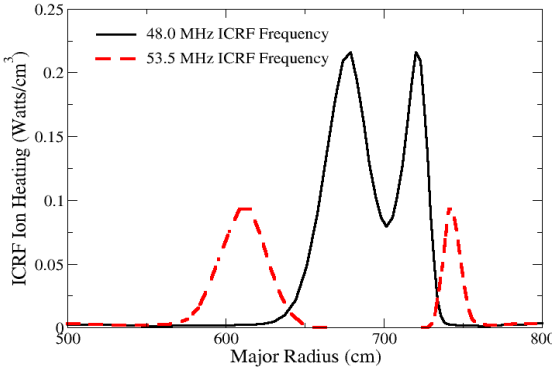

Figure 5 Dependence of heating location on ICRF Frequency

The fusion power production (including neutrons), obtained in three predictive PTRANSP simulations for the hybrid scenario, is shown in Fig. 6. The time interval considered in these simulations is a period of 500 seconds, and the pedestal temperature is taken to be 5 keV, a temperature consistent with EPED1 predictions. A new version of the Multi-Mode transport model is used in one of the simulations for which the power production results are presented. This transport model includes a drift resistive inertial ballooning mode module that is currently being validated against experimental data, including L-mode data. As a consequence of the resistive ballooning mode module, the multi-mode transport model, used in this simulation, is less stiff than the previously used mmm08 model. In the other fusion power results shown in Fig. 6, the GLF23 transport model is used. In one simulation, the momentum transport diffusivity, χ_i, is computed using the GLF23 model, and, in the other simulation, momentum transport is computed setting $\chi_\phi = \chi_i$. For the GLF23 simulations, the fusion power is still continuing to rise at 500 seconds and GLF23 simulations for longer periods of time will yield higher values of fusion power and thus of fusion *Q*. Because of the relative stiffness of the Multi-Mode and GLF23 transport models, reducing the auxiliary heating results in about the same fusion power production but a correspondingly higher fusion *Q*. This ability to increase fusion *Q* by decreasing the auxiliary heating, while the fusion power remains roughly constant applies to all of the scenarios. However, in the steady state scenario the injected power is required since this power produces the necessary current drive.

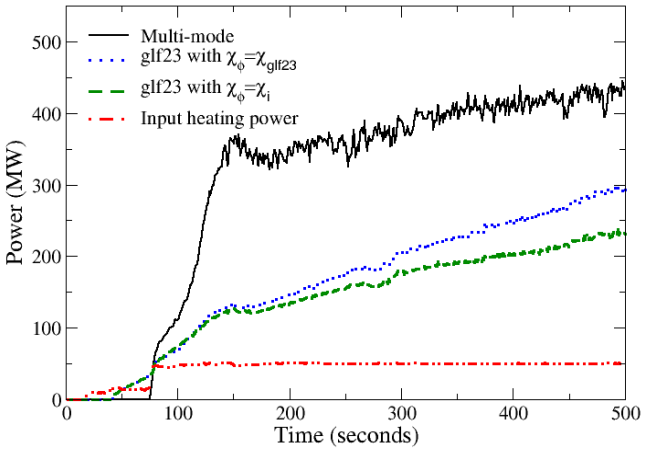

Figure 6 Fusion and Input power vs time

Transport Model	Fusion Q (500 s)
GLF23 with $\chi_\phi = \chi_i$	4.6
GLF with $\chi_\phi = \chi_{GLF}$	5.8
Multi-Mode	8.6

[1] F.D. Halpern, *et al.*, Phys. Plasmas **15**, 062505 (2008); R.V. Budny, *et al.*, Nucl. Fusion **48,** 075005 (2008)

[2] H. P. Summers *et al.*, AIP Conf. Proc. **901**, 239 (2007); http://open.adas.ac.uk

[3] P.B. Snyder *et al.*, Phys. Plasmas **16**, 056118 (2009)